Electronic Supplementary Material (ESI) for Nanoscale.

Supporting Information

Highly Sensitive and Wide-detection Range Pressure Sensor Constructing on Hierarchical Structure Conductive Fabric as Human-Machine Interface

Tao Chen[#a], Shao-Hui Zhang[#b], Qi-Hang Lin[a], Ming-Jiong Wang[a], Zhan Yang*[a], Yun-Lin Zhang[a], Feng-Xia Wang*[a], Li-Ning Sun[a]

[a]*Jiangsu Provincial Key Laboratory of Advanced Robotics, School of Mechanical and Electric Engineering, Soochow University, Suzhou 215123, China.*

[b]*Suzhou Institute of Nano-tech and Nano-bionics, Chinese Academy of Sciences, Suzhou 215123, China.*

Corresponding Author

wangfengxia@suda.edu.cn

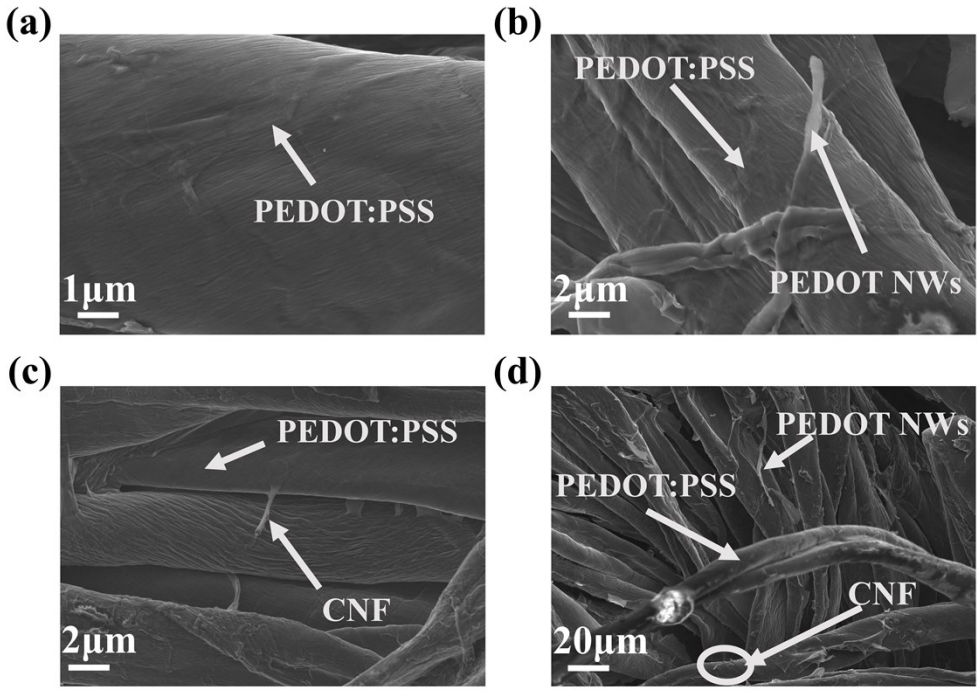

Figure S1 The SEM images of the hierarchical structured conductive fabric based on (a) PEDOT: PSS, (b) PEDOT: PSS/PEDOT NWs (c) PEDOT: PSS/CNF and (d) PEDOT: PSS/PEDOT NWs/CNF.

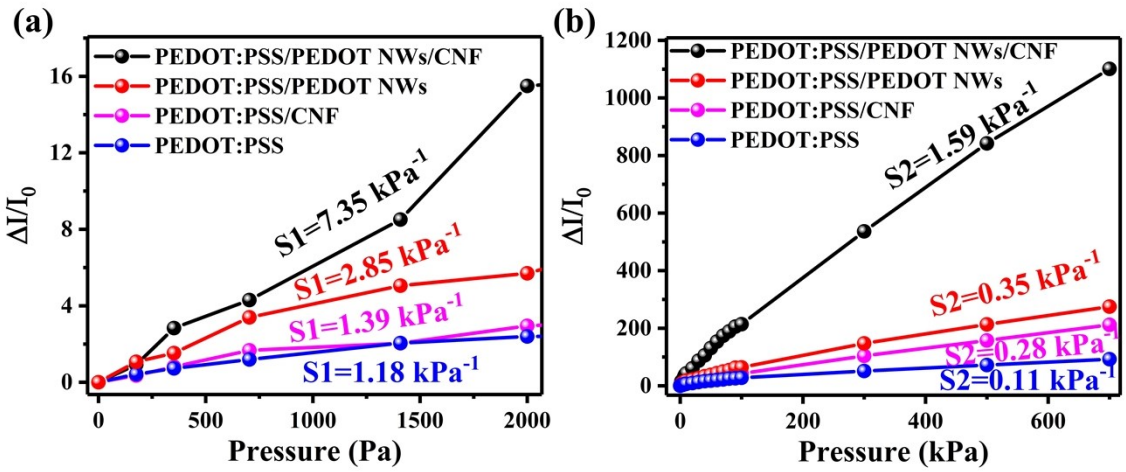

Figure S2 Different pressure regions (a) (less than 2kPa) and (b) (100kPa-700kPa) Sensitivity comparison of the four combinations of PEDOT:PSS, PEDOT NWs, and CNF materials.

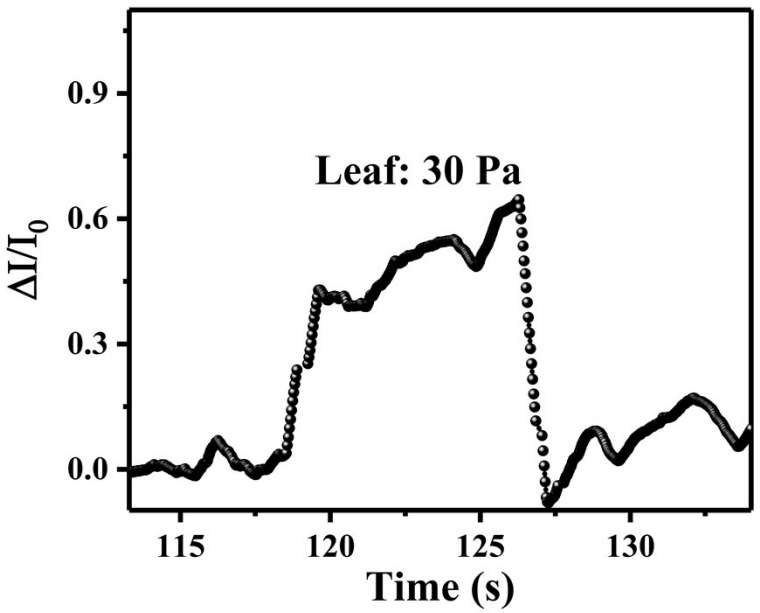

Figure S3 The relative current change of the pressure sensor based on conductive fabric under a leaf (30 Pa).

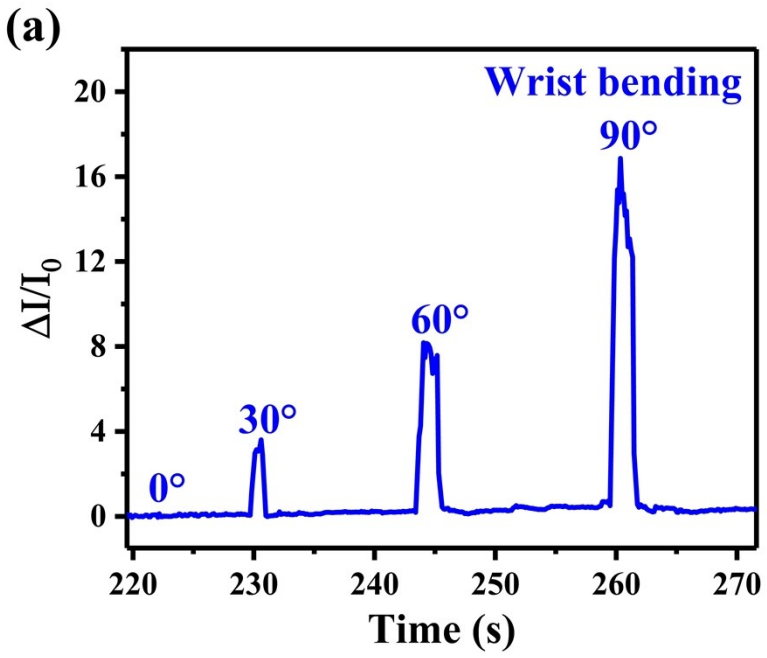

Figure S4 The relative current change of the pressure sensor based on the conductive fabric when the wrist is bent at different angles (0°, 30°, 60°, 90°).

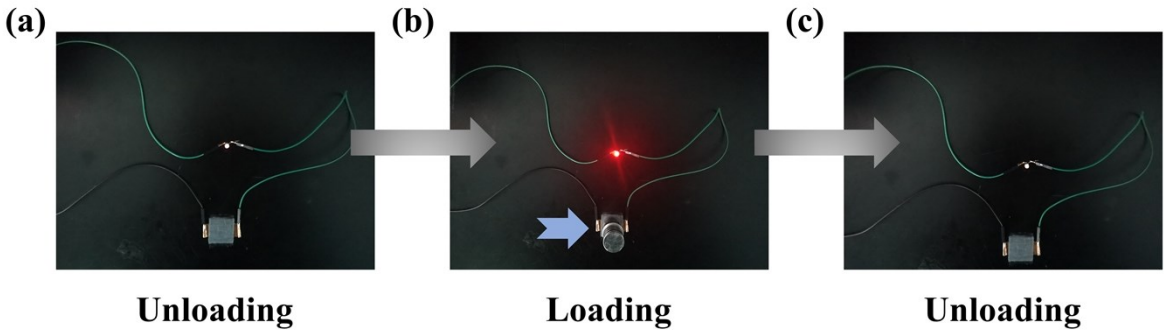

Figure S5 The change in brightness of LED light by loading on the fabric-based sensor.

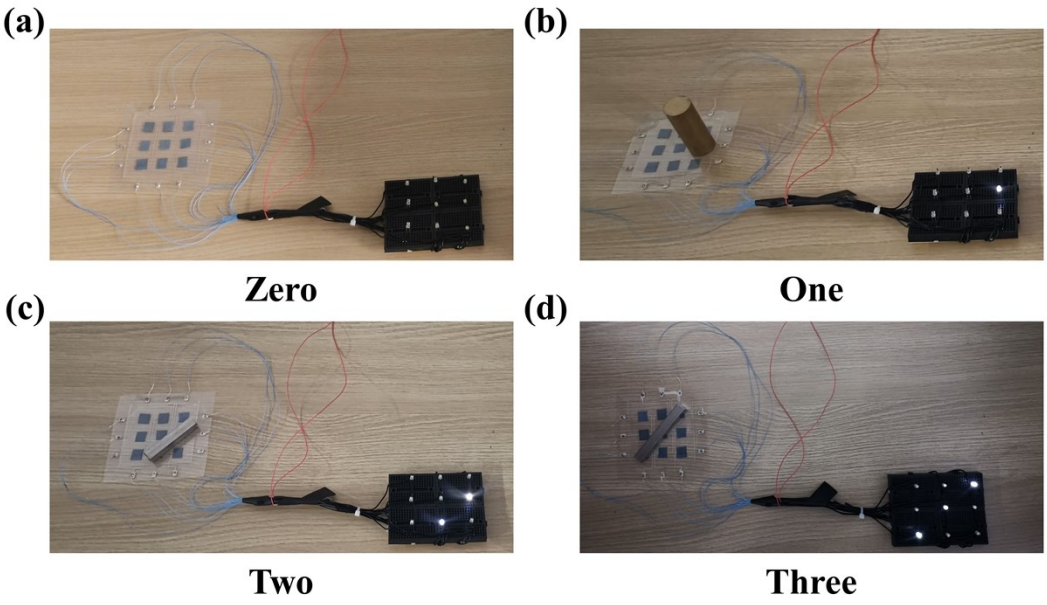

Figure S6 The picture of LED arrays and sensor arrays with different subjects and directions. The numbers below the picture refers to the number of the lighted LEDs.

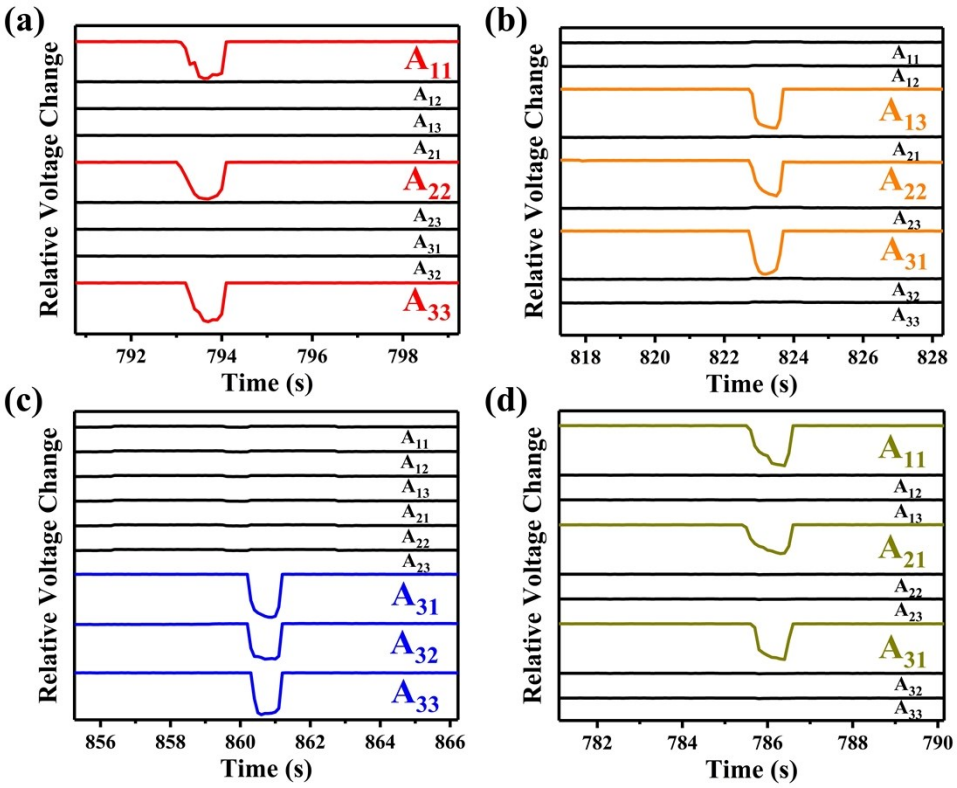

Figure S7 The change of voltage signal of the sensor array when a rectangular object is placed in the diagonal position of the sensor arrays. A_{11}-A_{33} represent the sensor on different position, as shown in the Figure 8a.

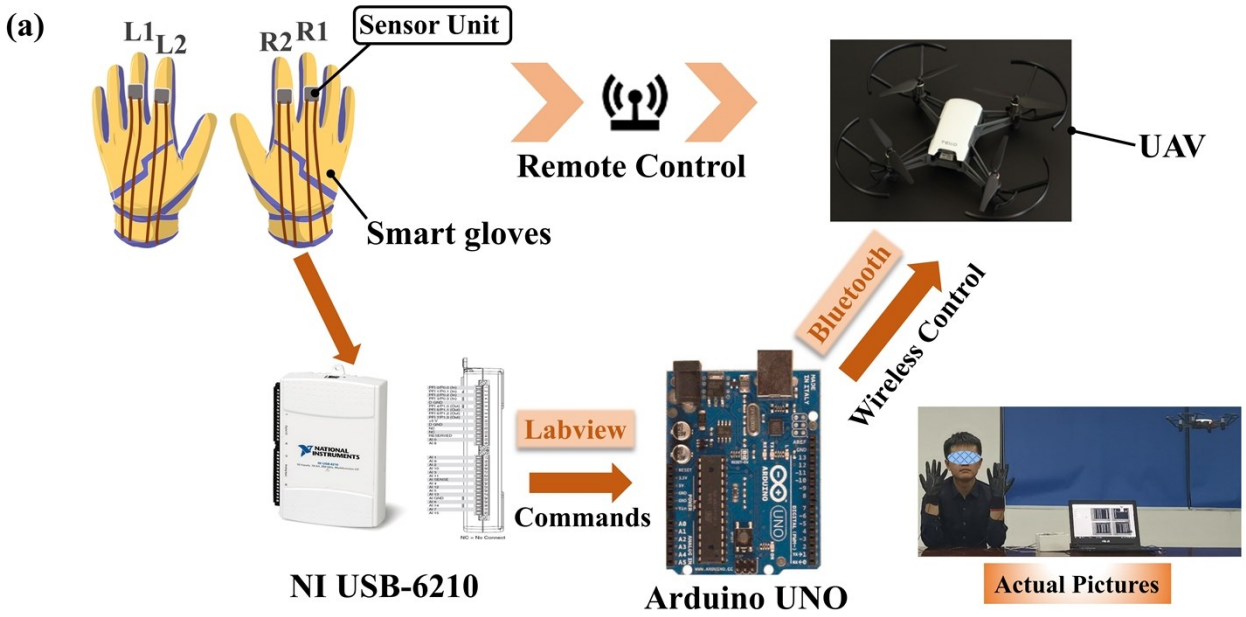

Figure S8 The diagram and work principle of the smart gloves based on the arrayed pressure sensor with PPCF for the control of unmanned aerial vehicle. The inset is the actual picture of the smart gloves.

Table S1 Comparison the performances of pressure sensors based on reported conductive fabric materials

Materials/Structures	Device type	Sensitivity	References
Graphene/polyamide	Piezoresistive	<0.3 kPa, 2.34 kPa^{-1} 0.3–80 kPa, 0.28 kPa^{-1}	S1
Graphene-Silk	Piezoresistive	<140kPa, 0.4 kPa^{-1}	S2
MXene-Textile	Piezoresistive	<29 kPa, 3.844 kPa^{-1} 29–40 kPa, 12.095 kPa^{-1}	S3
RGO/SWCNT-Fabric	Piezoresistive/Strain	1.27-12.7 kPa, 0.012kPa^{-1} 12.7-63.5 kPa, 0.002 kPa^{-1} 63.5-254 kPa, 0.724 MPa^{-1}	S4
CNT-cotton Textile	Piezoresistive	<3.5kPa, 14.4 kPa^{-1} 3.5 – 15 kPa, 7.8 kPa^{-1}	S5
Ag NWs-Textiles	Piezoresistive/Strain	<0.2 kPa, 1.03 kPa^{-1} 0.2–2kPa, 0.28 kPa^{-1} 6–10kPa, 0.9% kPa^{-1}	S6
PEDOT/CNF-fabric	Piezoresistive	<2 kPa, 15.78 kPa^{-1} 200-700 kPa, 1.5 kPa^{-1}	This work

S References

1. F. Yin, J. Yang, H. Peng and W. Yuan, *J. Mater. Chem. C*, 2018, **6**, 6840-6846.
2. Y. Liu, L.-Q. Tao, D.-Y. Wang, T.-Y. Zhang, Y. Yang and T.-L. Ren, *Appl. Phys. Lett.*, 2017, **110**, 123508.
3. T. Li, L. Chen, X. Yang, X. Chen, Z. Zhang, T. Zhao, X. Li and J. Zhang, *J. Mater. Chem. C*, 2019, **7**, 1022-1027.
4. S. J. Kim, W. Song, Y. Yi, B. K. Min, S. Mondal, K.-S. An and C.-G. Choi, *ACS Appl. Mater. Interfaces*, 2018, **10**, 3921-3928.
5. M. Liu, X. Pu, C. Jiang, T. Liu, X. Huang, L. Chen, C. Du, J. Sun, W. Hu and Z. L. Wang, *Adv. Mater.*, 2017, **29**, 1703700.
6. S. Chen, S. Liu, P. Wang, H. Liu and L. Liu, *JMatS*, 2017, **53**, 2995-3005.